Compositional analysis of Si nanostructures: SIMS–3D tomographic atom probe comparison

2007 Semicond. Sci. Technol. 22 S127

(http://iopscience.iop.org/0268-1242/22/1/S30)

INSTITUTE OF PHYSICS PUBLISHING SEMICONDUCTOR SCIENCE AND TECHNOLOGY

Semicond. Sci. Technol. **22** (2007) S127–S131 doi:10.1088/0268-1242/22/1/S30

Compositional analysis of Si nanostructures: SIMS–3D tomographic atom probe comparison

K Thompson[1], J H Bunton[1], J S Moore[2] and K S Jones[2]

[1] Imago Scientific Instruments, 6300 Enterprise Ln. Suite 100, Madison, WI 53719, USA
[2] University of Florida, SWAMP Group, Gainesville, FL, USA

Received 13 May 2006, in final form 23 August 2006
Published 5 December 2006
Online at stacks.iop.org/SST/22/S127

Abstract

3D atom probe tomography (APT) is introduced as a powerful compositional and spatial analytical tool for SiGe nanostructures. Compositional analysis of SiGe structures demonstrates that the location and identity of Si, Ge and B atoms can be detected in three dimensions. Superior sensitivity at Si–SiGe–Si interfaces is specifically witnessed by both the quantification of Ge accumulation at an interface (14% by atom probe versus 9% by SIMS) and a slope roll-off of ∼1 nm/decade for atom probe compared to ∼7 nm/decade for the corresponding SIMS analysis. Additionally, APT provides chemical roughness measurements of buried interfaces. In a specific case, a Si–SiGe–Si interface had a measured roughness of 0.47 nm at the Si–SiGe leading edge and 0.26 nm at the SiGe–Si trailing edge.

(Some figures in this article are in colour only in the electronic version)

1. Introduction

As SiGe finds broader use in nano-devices, greater attention has been focused on understanding the capabilities and limitations of techniques for compositional analysis [1–3]. As feature length scales in these devices shrink below 10 nm, variations in the chemical composition of these devices—specifically the location of dopant atoms and the quality of interfaces between regions—may have a significant impact on the final electrical characteristics of the device. As a result, it is important to monitor, as near to the atomic level as possible, the chemical composition of these nanostructures.

The addition of high speed laser pulsing and a Local Electrode™ geometry has transformed the 3D atom probe into a characterization tool that is capable of analysing Si-based nanostructures on an atom-by-atom basis [4–6]. In order to demonstrate the applicability of atom probe tomography (APT) to the study of SiGe, doped and undoped SiGe structures were successfully analysed with a laser-assisted local electrode atom probe. The results correlate favourably with secondary ion mass spectrometry (SIMS).

2. Experimental apparatus

All atom probe experiments were run in the LEAP3000X™ system from Imago Scientific Instruments [4]. Field evaporation was achieved with an ultra-fast pulsed laser system. With a duty cycle of 250 kHz and an evaporation rate of 4%, approximately 36 million atoms h^{-1} were collected. For a 50 nm analysis radius this resulted in a data collection rate of 3 nm min^{-1}. The base temperature of the sample was maintained at 40 K and the analysis chamber pressure was kept lower than 10^{-8} Pa. The depth resolution of the atom probe ranges between 0.2 and 0.4 nm depending on the material system analysed [4]. The measurement error of atomic concentrations depends on Poisson statistics, which is a function of the total number of atoms counted within each volume of interest [4–6].

The SIMS was performed in a PHI quadrupole system with a 1 keV Cs^+ beam at a 60° angle. The SIMS spot size was 25 microns in radius. No oxygen flood was utilized, and an electron flood gun provided charge neutralization. The error in quantification of Ge and B by SIMS was less than 0.1%. The SIMS analysis was performed opposite the growth rate for each of the film stacks discussed.

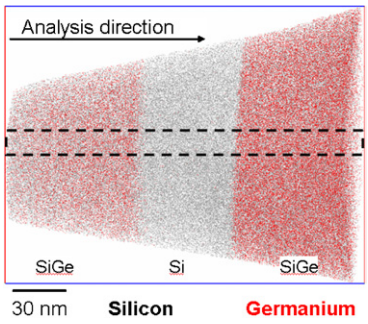

Figure 1. 3D atom map of a SiGe–Si–SiGe test structure. For clarity, the image is shown in 2D projection. Si atoms: grey dots. Ge atoms: black dots.

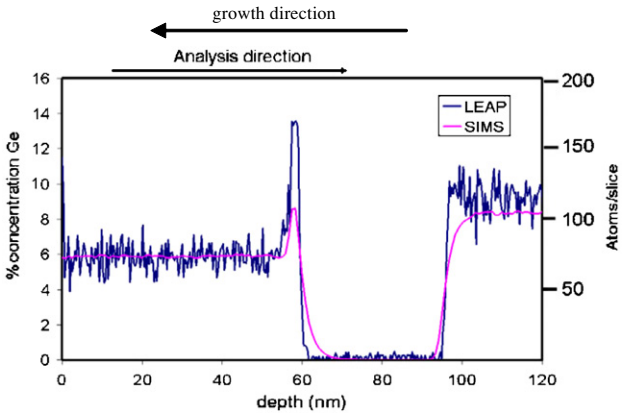

Figure 2. 1D composition profile for the atom map in figure 1.

Samples were prepared in an FEI Nova-235 dual beam FIB. The region of interest was protected by e-beam assisted Pt deposition in the FIB with an e-beam energy of 2 keV. The samples were extracted using the FIB lift-out and mount technique described elsewhere [7, 8]. The extracted samples were milled into an appropriate atom probe tip form with 75 nm radius of curvature followed by a low keV Ga clean-up mill, also as discussed elsewhere [9, 10].

3. Compositional analysis

The effectiveness of atom probe tomography at analysing SiGe nanostructures was evaluated on three distinct materials systems. The successful analysis of these systems demonstrates the capability of atom probe analysis to obtain spatial and compositional information concerning a generic SiGe system.

3.1. SiGe–Si–SiGe

The first system consisted of a SiGe–Si–SiGe multilayer stack deposited by CVD deposition. This stack was analysed in the laser atom probe and correlated with the SIMS analysis. The resulting 3D atom map is shown in figure 1. For visual clarity, the image is shown in 2D projection. The Si atoms (light grey dots) and the Ge atoms (dark black dots) are shown at 2% and 20% of the actual concentration respectively. A 1D composition profile of the structure is extracted from the 3D

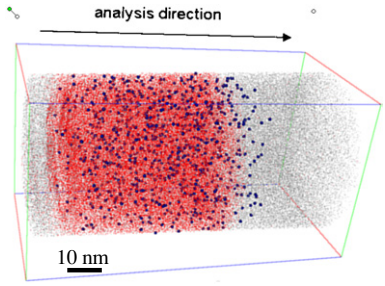

Figure 3. 3D atom map of a B-doped SiGe layer. B atoms are rendered as blue spheres, sized larger for emphasis. Si atoms: grey dots. Ge atoms: black dots.

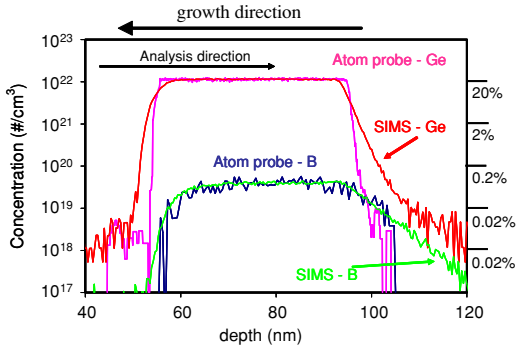

Figure 4. 1D composition profile for atom map in figure 3 along with SIMS correlation.

atom-map by creating an analysis cylinder along the analysis (depth) direction. The cylinder utilized was 5 nm in radius and sliced into 0.33 nm thick discs. The atoms within each slice were tabulated to determine the atom concentration as a function of depth. The 1D composition, along with SIMS comparison, is shown in figure 2. The axes in figure 2 are shown in both %concentration (SIMS and APT) and number of atoms per slice (APT only). The measurement error for the Ge concentration as measured by APT is $\pm 0.7\%$; as measured by SIMS, it is $<0.1\%$.

Both SIMS and APT successfully quantified the Ge concentration in each SiGe layer (6% for the upper layer and 9% for the lower) and measured the thickness of the Si layer in between the SiGe layers. The atom probe technique offers a superior depth resolution of the buried interface, with a slope roll-off of $\sim$1 nm/decade, compared to 7 nm/decade with this SIMS analysis. Additionally, both techniques have detected an accumulation of Ge at the Si–SiGe interface. The peak accumulation measured in the atom probe was 14% versus 9% measured by SIMS; a difference which exceeds the experimental error.

3.2. Si–SiGe:B–Si

The second material analysed was a B-doped SiGe layer, situated between two undoped Si layers. The resulting 3D atom map is shown in figure 3 where 2% of the Si atoms (grey dots), 20% of the Ge atoms (dark black dots) and 100% of the B dopant atoms (large spheres) are shown. It is evident from the atom map that a small amount of B diffusion, from the SiGe layer and into the underlying Si, has occurred. A 1D composition profile in the analysis direction was obtained

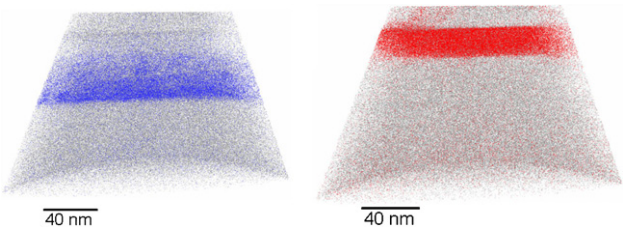

Figure 5. 3D atom map of a Si–SiGe–Si:B layer. Si atoms: grey dots. Visualizations of the B (left) and Ge atoms (right) are shown in separate maps for clarity.

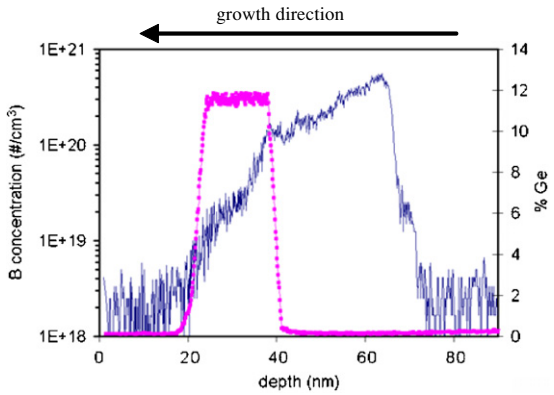

Figure 6. 1D composition profile for atom map in figure 5.

by creating an analysis cylinder 25 nm in radius, cutting the cylinder into 1 nm discs and tabulating the atoms within each slice. On average there were ∼75 B atoms/slice in the SiGe region for a dopant concentration of 3.9×10^{19} cm^{-3} $\pm$ 4×10^{18} cm^{-3}. This compositional analysis is shown in figure 4 along with the SIMS correlation. The 1D composition profiles verify that there was some diffusion of B into the underlying Si and also show a slight rarification of Si towards the top of the SiGe layer. Because B has diffused into the underlying Si and not into the top Si layer, it is likely that the B diffusion occurred during the SiGe deposition process.

3.3. Si–SiGe–Si:B

The third analysis was of a B-doped Si layer directly below an undoped SiGe layer. The resulting 3D atom map is shown in figure 5 with the corresponding 1D compositional analysis shown in figure 6. The analysis field of view on this sample was ∼170 nm in diameter, which is more than large enough to contain most nanostructures of interest. The B dopant concentration rises to a maximum level of 5×10^{20} cm^{-3}. There appears to be considerable diffusion of B from the underlying Si layer into the SiGe layer.

3.4. Analysis

While SIMS and atom probe correlate well, there are some distinct differences between the two techniques. These differences are attributed to the different mechanisms utilized to extract atoms from the sample. The laser atom probe removes atoms one at a time by the dual mechanism of electric field ionization followed by pulsed field evaporation [11–14]. Mass detection occurs by a time-of-flight instrument measurement and atom species are collected with equal efficiency across the entire mass range. The implication is that a single atom probe analysis provides the location and chemical identification of each species of atom with no need for multiple analyses. The SIMS analysis employs an energetic ion beam that actively sputters atoms from the surface of the material. This sputter removal process mixes the top several nm of the exposed surface. Additionally, the energetic primary ion beam drives certain atomic species deeper into the sample, inhibiting the characterization of sharp composition gradients [15–19]. The result is an exaggeration of the transition between two layers or accumulation artefacts at this interface. It is also not uncommon to see aberrations in the B profile during a SIMS analysis of SiGe [20, 21]. Ge is best collected with a Cs^+ primary ion beam while O_2^+ is typically utilized for B detection. Additionally, the sputter and ionization rate of B varies as a function of Ge concentration. This can typically be corrected for but complicates—thereby adding a level of uncertainty to—the analysis. For this reason, SIMS analysis of B-doped SiGe typically requires at least two analyses, which are then overlaid. In order to improve profiling accuracy, one may also perform a back-side SIMS analysis to create a comparison of the composition profile at important interfaces [18, 19].

The comparative advantages of both SIMS and atom probe are demonstrated in the analyses discussed. In all cases, the atom probe provided superior slope roll-off at the interface. This is particularly evident in figures 2 and 4 for the quantification of the Ge concentration. Ion mixing of the sputter surface during SIMS has blurred the interfaces between the SiGe and Si layers, and the Ge is clearly being driven into the wafer at the SiGe–Si interface. With regard to the undoped SiGe–Si–SiGe structure, figure 2, both the atom probe and the SIMS analysis quantified an accumulation of Ge at the SiGe–Si interface. However, APT quantifies a markedly higher concentration of Ge (14% $\pm$ 0.7%) at the interface as compared to SIMS (9%). Accumulation artefacts such as these are known to occur in SIMS analysis, and back-side SIMS may be required to verify the accumulation [18, 19]. Without a third analysis technique, it is difficult to make a strong statement as to whether this accumulation is 14% or 9%. However, because the atom probe technique is inherently more sensitive to abrupt interfaces, one can argue that the 14% peak Ge accumulation at the interface measured by APT is more likely than the 9% measured by SIMS.

Finally, the atom probe quantification of the dopant atoms displays some variation, figure 4, across a region of uniform B doping. This variation is, in fact, the actual variance in B atoms throughout the non-homogeneously doped structure. Consider the analysis cylinder dimensions (25 nm radius, 1 nm thick slice) used to tabulate the 1D composition profile. There are, on average, 75 dopant atoms per slice. Poisson statistics indicate a variation of $\pm$8 dopant atoms per slice. Dividing the number of dopant atoms (75) by the volume of the slice (1963 nm^3), determines the volume concentration and variation stated in section 3.2 of 3.9×10^{19} cm^{-3} $\pm 4 \times 10^{18}$ cm^{-3}. While the use of log scales somewhat obscures the magnitude of this variance, it represents the actual

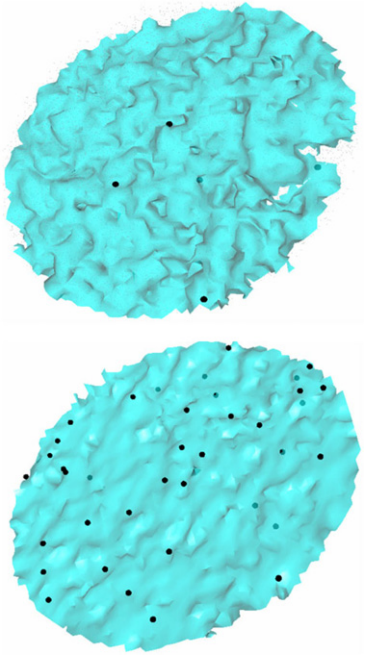

Figure 7. Chemical roughness analysis for the Si–SiGe:B–Si system. The top (leading Si–SiGe) and bottom (trailing SiGe–Si) surfaces had a roughness of 0.47 nm and 0.26 nm respectively. The dopant atoms that decorate the surface (i.e. are within 0.5 nm of the surface) are shown as dark-coloured spheres.

nanoscale non-uniformity in the arrangement of dopant atoms within the material. With regards to 1D compositional analysis it also represents a pragmatic lower limit for dilute species detection in the atom probe. The solution to this limit is to employ a larger area, or field of view, for the analysis. SIMS takes this to the extreme with an area ∼50 000 times larger. The result is a virtual elimination of atomic location variance and a superior sensitivity to dilute species during the SIMS analysis.

4. Interface analysis

In addition to compositional analysis, the knowledge of atom locations allows one to perform a careful analysis of the interface between specified layers. Specifically, the interface between any two layers was analysed by constructing an iso-chemical contour across the buried interface for the dataset shown in figure 3. This isocontour was defined at the point where the local concentration of a given species of atom had risen above or had fallen below a specified value. The average roughness of the interface was then calculated using the ASME B46.1-2002 standard. Because this technique relies upon an analysis of the variation in chemical concentration, it provides a 'chemical-roughness'—which may be different from the physical roughness measured by atomic force microscopy (AFM).

This chemical roughness calculation was performed for the Si–SiGe:B–Si system of section 3.2. The associated isocontour maps are shown in figure 7. The leading Si–SiGe and trailing SiGe–Si interfaces were defined where the Ge concentration crossed the 8% concentration threshold. In this case, chemical roughnesses of 0.47 nm and 0.26 nm were calculated at the leading Si–SiGe and trailing SiGe–Si edges respectively. In addition, the distribution of B atoms is shown (dark spheres) across these surfaces. While there is considerable B decoration along the surface of the trailing edge, there is virtually no dopant decoration of the leading edge. This matches well with the 1D compositional analysis, which shows a rarification of B at the leading Si–SiGe layer and a migration of dopant atoms into the underlying Si at the end of the SiGe layer.

5. Conclusion

These experiments demonstrate the applicability of the 3D tomographic atom probe as a compositional tool for analysis of SiGe nanostructures. The technique correlates favourably with measurements made on these same structures using SIMS. The ability to map the location and to determine the identity of atoms in 3D space within a SiGe nanostructure gives rise to sensitive compositional analysis at interfaces without the artefacts associated with SIMS. Furthermore, the knowledge of atom positions allows for the calculation of the chemical roughness of buried interfaces and for the visualization of dopant atom decoration along these interfaces. Expanded use of this technique should allow for the mapping of entire SiGe nanostructures which would contain 2D and 3D distributions of dopant atoms along with other site-specific features of interest.

Acknowledgments

The authors gratefully acknowledge the work of everyone involved with this project. Specifically the engineering team—Dan Lenz, A Patel, T Payne, J Shephard, E Strennen, D Sund—, software analysis—D Beerman, B Geiser, T Kunicki, E Oltman—and applications lab—M Ali, R Alvis, D Lawrence, D Olson, R O'Neill—teams.

References

[1] Wang G, Yuan H C and Ma Z 2006 *IEEE Electron Device Lett.* **27** 371
[2] Ma Z and Jiang N 2006 *IEEE Trans. Electron Device* **53** 875
[3] Krecar D, Rosner M, Draxler M, Bauer P and Hutter H 2006 *Anal. Bianal. Chem* **384** 525
[4] Kelly T F *et al* 2004 *Microsc. Microanal.* **10** 373
[5] Thompson K, Booske J H, Larson D J and Kelly T F 2005 *Appl. Phys. Lett.* **87** L05-1775
[6] Thompson K, Bunton J H, Kelly T F and Larson D J 2006 *J. Vac. Sci. Technol.* B **24** 421
[7] Miller M K, Russell K F and Thompson G B 2005 *Ultramicroscopy* **102** 287–98
[8] Lawrence D, Thompson K, Larson D and Gorman B 2006 Site-specific lift out sample preparation technique for atom probe analysis *Proc. Microscopy and Microanalysis (Chicago, IL)*
[9] Larson D J, Wissman B D, Martens R L, Viellieux R J, Kelly T F, Gribb T T, Erskine H F and Tabat N 2001 *Microsc. Microanal.* **7** 24–31
[10] Thompson K, Gorman B, Larson D J, van Leer Brandon and Hong Liang 2006 Minimization of Ga induced FIB damage using low energy clean-up *Proc. Microscopy and Microanalysis (Chicago, IL)*

[11] Tsong T T 1990 *Atom-Probe Field Ion Microscopy: Field Ion Emission, and Surfaces and Interfaces at Atomic Resolution* (Cambridge: Cambridge University Press)
[12] Müller E W, Panitz J A and Mclane S B 1968 *Rev. Sci. Instrum.* **39** 83
[13] Panitz J A 1982 *J. Phys. E: Sci. Instrum.* **15** 1281
[14] Miller M K, Cerezo A, Heatherington M G and Smith G D W 1996 *Atom Probe Field Ion Microscopy* (Oxford: Oxford Science Publications)
[15] Aoki T, Chiba S, Matsuo J, Yamada I and Biersack J P 2001 *Nucl. Instrum. Methods Phys. Res.* B **180** 312
[16] Yang M H, Mount G and Mowat I 2006 *J. Vac. Sci. Technol.* B **24** 428–432
[17] Vandervorst W, Bennett J, Huyghebaert C, Conard T, Gondran C and De Witte H 2004 *Appl. Surf. Sci.* **231–2** 618
[18] Janssens T, Pawlak M A, Kittl J A, Fouchier M, Lauwers A, Kottantharayil A and Vandervorst W 2006 Dopant profiling in Ni_xSi_{1-x} gates with secondary-ion-mass spectroscopy *J. Vac. Sci. Technol.* B **24** 399
[19] Tomita M, Hongo C, Suzuki M, Takenaka M and Murakoshi A 2004 *J. Vac. Sci. Technol.* B **22** 117
[20] Bennett J, Kohli P, Wise R, Rodder M, Yu S, Cleavelen R, Pas M, Braithwaite G, Currie M T and Lochtefeld A 2004 *Proc. 206th Meeting of the Electrochemical Society* p 1306
[21] Krecar D, Rosner M, Draxler M, Bauer P and Hutter H 2005 *Appl. Surf. Sci.* **252** 123